CO oxidation on Gold-supported Iron Oxides: New Insights into Strong Oxide-Metal Interactions

Liang Yu,[1,2] Yun Liu,[1,2] Fan Yang,[1,2] Jaime Evans,[3] Jose A. Rodriguez,[4*] and Ping Liu[4*]

1 Collaborative Innovation Center of Chemistry for Energy Materials, Xiamen University, Xiamen 361006, China

2 State Key Laboratory of Catalysis, Dalian Institute of Chemical Physics, Dalian 116023, China

3 Facultad de Ciencias, Universidad Central de Venezuela, Apartado 20513, Caracas 1020-A, Venezuela

4 Chemistry Department, Brookhaven National Laboratory, Upton, New York 11973, United States

Computational details

Based on the periodicity of bright spots and moiré pattern from STM measurements, the FeO(111) bilayer on Au was simulated with a slab model of Au(111) in a 12×12 supercell (35.4Å × 35.4Å) of pre-optimized gold lattice; the FeO bilayer with lattice distance of 3.05Å was extracted from the optimized FeO bulk and rotated by 4.3 degree along the z axis with respect to the gold lattice to match the periodicity of the supercell. The Fe_3O_4(111) overlayer on Au(111) was simulated with a supercell of 4×4 Au(111) slab supporting a 2×2 Fe_3O_4(111) slab. The Fe_2O_3(001) overlayer on Au(111) was simulated with a supercell of 5×5 Au(111) slab supporting a 3×3 Fe_2O_3(001) slab.

The phase change of FeO_x in dependence of the chemical potential of CO and O_2 was calculated based on the thermodynamic method reported in Ref 1. For two different phases on exposure to both CO and O_2, the redox reactions were considered, e.g.

Reduction reaction: $FeO_x + CO \rightarrow FeO_{x-1} + CO_2$

Oxidation reaction: $FeO_{x-1} + {}^1/_2O_2 \rightarrow FeO_x$

Under the equilibrium condition for FeO_x and FeO_{x-1} phases, the free energy changes for FeO_x reduction and FeO_{x-1} oxidation reaction are in equivalent, i.e. $\Delta G_{red}=\Delta G_{ox}$, in which,

$\Delta G_{red} = \mu(FeO_{x-1}) + \mu(CO_2) - \mu(FeO_x) - \mu(CO)$

$\Delta G_{ox} = \mu(FeO_x) - \mu(FeO_{x-1}) - {}^1/_2\mu(O_2)$

where μ is the chemical potential.

For the iron or iron compound phases, we use the DFT calculated total energy (E_{total}) as the chemical potential, i.e. $\mu(FeO_x) = E_{total}(FeO_x/Au) - E_{total}(Au)$.

For the gas phases, such as CO, O_2, and CO_2, the chemical potentialwas calculated as E_{total} + ZPE + Δμ, where $\Delta\mu = -TS + kT\ln(P/P^0)$, T is temperature, S is entropy, P is the partial pressure, P^0 is the standard atmosphere pressure, and ZPE is the zero point energy correction.

Results

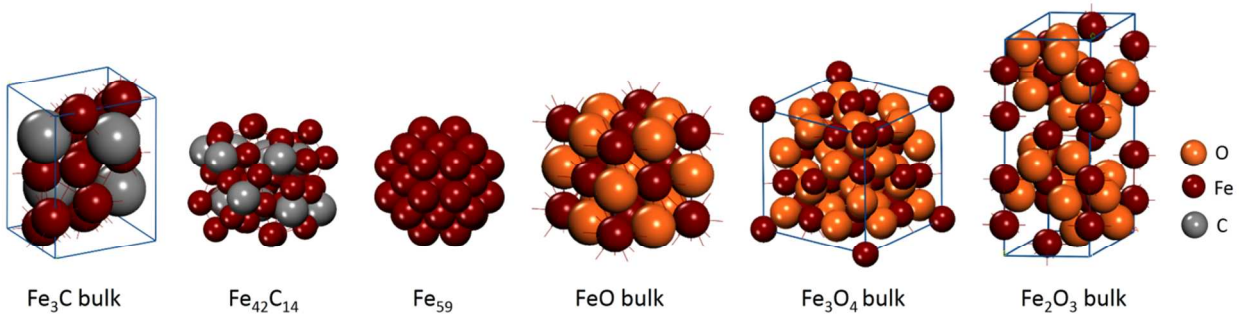

Figure S1. DFT-optimized structures of Fe_3C bulk, $Fe_{42}C_{14}$ cluster, Fe_{59} cluster, FeO bulk, Fe_3O_4 bulk, and Fe_2O_3 bulk.

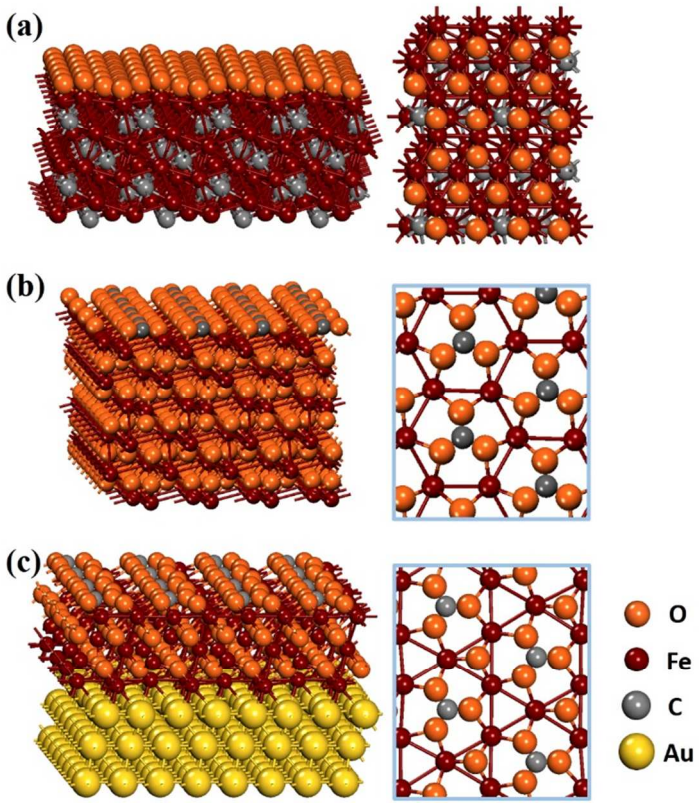

Figure S2. (a) $Fe_3C(001)$ surface fully covered by O_{ads} species. (b) $Fe_2O_3(001)$ surface and (b) terrace of $Fe_3O_4(111)$ overlayer on Au(111) passivated by surface carbonate structures. The right column is the top view of the surfaces.

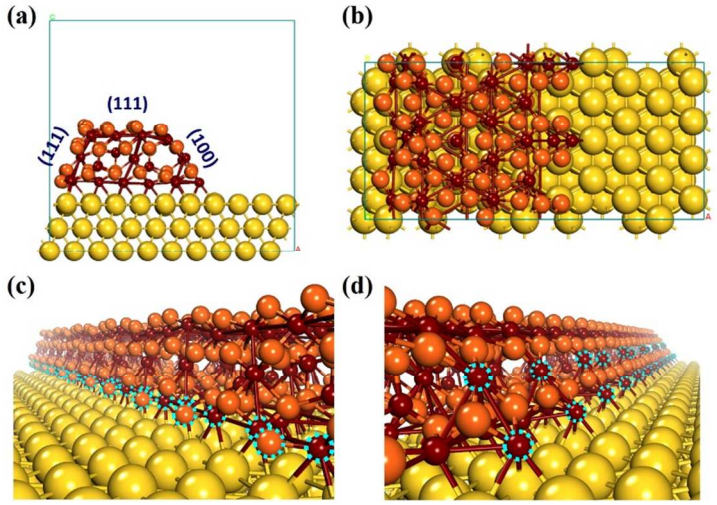

Figure S3. (a) Sectional view and (b) top view of the strip model of Fe_3O_4 on Au(111). Perspective view of (c) Fe_3O_4(111)/Au and (d) Fe_3O_4(100)/Au interfaces. The doted circles denote the active sites for CO oxidation.

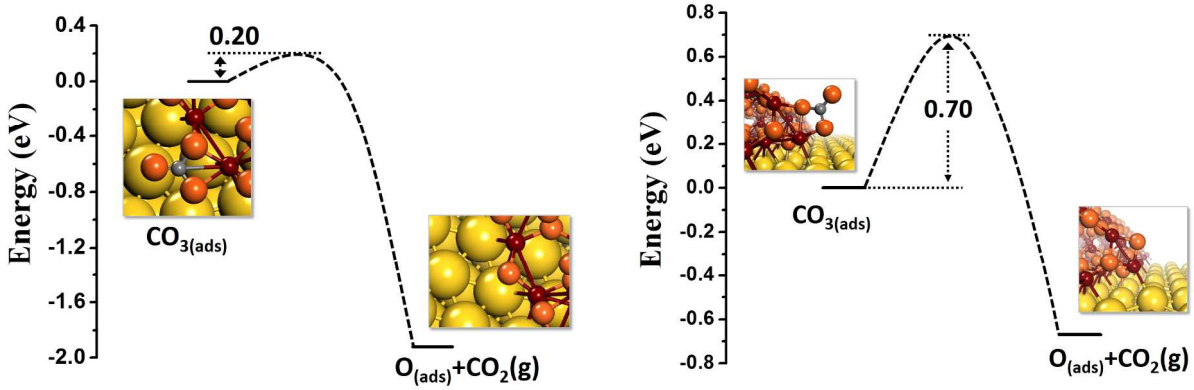

(a) (b)

Figure S4. Energetics and kinetics of carbonate formation at the interfacial sites of (a) Fe_3O_4(111)/Au and (b) Fe_3O_4(100)/Au. The entropy contributions at 575K for the steps involving gas phase CO, O_2 and CO_2 were included.

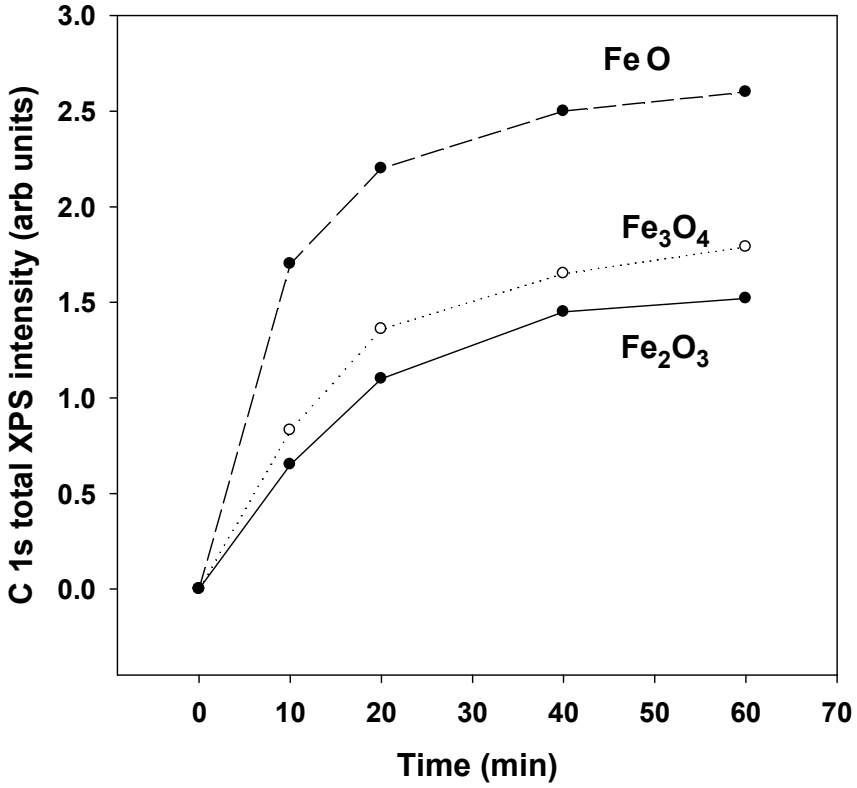

Figure S5. Accumulation of carbon-containing species on FeO/Au(111), Fe_3O_4/Au(111) and Fe_2O_3/Au(111) as a function of time upon exposure to a mixture of 5 Torr of CO and 5 Torr of O_2 at 575 K.

Reference

[1] K. Reuter and M. Scheffler, *Physical Review B*, **2001**, *65*, 035406.